# Bubble-bubble interaction: A potential source of cavitation noise

Masato Ida*

*Center for Computational Science and E-systems, Japan Atomic Energy Agency, Higashi-Ueno, Taito-ku, Tokyo 110-0015, Japan*

(Received 22 July 2008; revised manuscript received 16 October 2008; published 14 January 2009)

The interaction between microbubbles through pressure pulses has been studied to show that it can be a source of cavitation noise. A recent report demonstrated that the acoustic noise generated by a shrimp originates from the collapse of a cavitation bubble produced when the shrimp closes its snapper claw. The recorded acoustic signal contains a broadband noise that consists of positive and negative pulses, but a theoretical model for single bubbles fails to reproduce the negative ones. Using a nonlinear multibubble model, we have shown here that the negative pulses can be explained by considering the interaction of microbubbles formed after the cavitation bubble has collapsed and fragmented: Positive pulses produced at the collapse of the microbubbles hit and impulsively compress neighboring microbubbles to generate reflected pulses whose amplitudes are negative. Discussing the details of the noise generation process, we have found that no negative pulses are generated if the internal pressure of the reflecting bubble is very high when hit by a positive pulse.

DOI: 10.1103/PhysRevE.79.016307 PACS number(s): 47.55.dp, 47.55.dd

## I. INTRODUCTION

In a recent paper, Versluis *et al.* reported that the snapping shrimp (*Alpheus heterochaelis*) living in the ocean can generate a cavitation bubble by rapidly closing its large snapper claw [1]. The rapid closure produces a negative pressure in seawater, by which cavitation nuclei (e.g., air microbubbles) are explosively expanded to a radius of a few millimeters. The cavitation bubble then collapses violently and emits a loud acoustic noise. The experimentally recorded acoustic signal presented in Ref. [1] consists of a strong (positive) pressure pulse, clearly produced at the bubble collapse, and a subsequent broadband noise [2]. A single-bubble theoretical model (the Keller-Miksis equation) succeeded in reproducing the strong pressure pulse (and a weak precursor signal) but failed to describe the broadband noise. Versluis *et al.* stated that the broadband noise is partly due to the reflection of the pressure pulse at nearby aquarium walls. However, the broadband noise begins earlier than the arrival of the reflected wave, immediately after the bubble collapse.

The broadband noise appears to consist of both positive and negative pressure pulses (or steep spikes) whose amplitudes are smaller than the first strong pulse. As demonstrated in Ref. [1] and shown below, however, the single-bubble model cannot describe negative pulses. A key to resolving this inconsistency is given from an image recording of the cavitation bubble. In a series of high-speed images, it was found that at collapse the single cavitation bubble breaks apart through the surface instability and then an opaque cloud of microbubbles appears [1]. The bubble cloud seems to grow and finally dissolve away.

We hypothesize that the interaction between the microbubbles through pressure pulses is a source of the negative pulses involved in the broadband noise. It is known that bubbles undergoing volume change interact with each other through the pressure waves that they emit. Bubble-bubble interaction of this type leads to a variety of phenomena, including attraction and repulsion between bubbles [5–10], filamentary structure formation [11], change of eigenfrequencies [12], superresonances [13], emergence of transition frequencies [10,14], avoided crossing of resonance frequencies [15], sound localization [16], and suppression of cavitation inception [17,18]. Because at generation the microbubbles are highly compressed, they must begin volume change (as observed) and emit pressure pulses at their collapse. Taking the bubble-bubble interaction through the pressure pulses into consideration, in this paper we suggest a possible origin of the negative pulses. Here we do not aim at providing a quantitative explanation, because the actual sizes and number density of the microbubbles are now unknown. We instead attempt to elucidate the basic mechanism of negative pulse generation, reducing the problem to the interaction of only two bubbles.

The rest of this paper is organized as follows. In Sec. II, the model equations and assumptions used in this study are introduced. Section III presents numerical and theoretical results and discussions of the pressure pulses emitted by interacting bubbles, and Sec. IV summarizes the results obtained.

## II. MODEL EQUATIONS

The theoretical model used in this study is the coupled Keller-Miksis equations [7,18], which describe the radial motion of two coupled spherical bubbles in a compressible liquid:

$$\left(1-\frac{\dot{R}_i}{c}\right)R_i\ddot{R}_i+\left(\frac{3}{2}-\frac{\dot{R}_i}{2c}\right)\dot{R}_i^2 = \frac{1}{\rho}\left(1+\frac{\dot{R}_i}{c}\right)p_{s,i}+\frac{R_i}{\rho c}\frac{d}{dt}p_{s,i}-\sum_{j=1,j\neq i}^{2}\frac{1}{D_{ij}}\frac{d(R_j^2\dot{R}_j)}{dt}, \quad (1)$$

$$p_{s,i}\equiv p_{b,i}-\frac{2\sigma}{R_i}-\frac{4\mu\dot{R}_i}{R_i}-P_0 \quad \text{for } i=1,2, \quad (2)$$

where $R_i=R_i(t)$ is the instantaneous radius of bubble $i$, $D_{ij}$ is the center-to-center distance between bubbles $i$ and $j$, and the

*ida.masato@jaea.go.jp

 

overdots denote the time derivative $d/dt$. The surrounding liquid is assumed to be water with density $\rho=1000\ \mathrm{kg/m^3}$, viscosity $\mu=1.002\times10^{-3}\ \mathrm{kg/m\,s}$, sound speed $c=1500\ \mathrm{m/s}$, and surface tension $\sigma=0.0728\ \mathrm{N/m}$. The far-field pressure $P_0$ is assumed to be constant in time and equal to the atmospheric pressure, 0.1013 MPa. The gas in the bubbles is assumed to be a van der Waals gas (air) and the pressure inside bubble $i$ ($p_{b,i}$) is determined by

$$p_{b,i}=\left(P_0+\frac{2\sigma}{R_{i0}}\right)\left(\frac{R_{i0}^3-h_i^3}{R_i^3-h_i^3}\right)^{\kappa}, \tag{3}$$

where $R_{i0}$ is the ambient radius and $h_i$ is the hard-core radius ($R_{i0}/8.54$ for air [19]). The polytropic exponent of the gas, $\kappa$, is assumed to be equal to its specific heat ratio $\gamma$ (1.4 for air) because our interest is in the pressure pulses emitted at bubble collapse, where the bubble behavior is nearly adiabatic. We confirmed numerically that, even when the heat exchange between the bubbles and water is taken into account by, e.g., a switching method for $\kappa$ [20], the results are essentially the same as those shown below. The vapor pressure is neglected for simplicity. We do not consider mass exchange (i.e., evaporation and condensation, mass diffusion) and chemical reactions, which may occur inside the bubbles [21], since they are not essential for sound emission: As demonstrated in earlier work on single bubbles [22,23], models that do not take mass exchange and chemical reactions into account can describe bubble-emitted pressure waves with sufficient accuracy.

The last term of Eq. (1) describes the bubble-bubble interaction through the bubble-emitted pressure waves and acts as a driving force on bubble $i$. This term was derived from the following simple formula, which corresponds to an equation for the pressure wave emitted by a pulsating sphere:

$$p_i=\frac{\rho}{r_i}\frac{d(R_i^2\dot{R}_i)}{dt}=\frac{\rho}{r_i}(2R_i\dot{R}_i^2+R_i^2\ddot{R}_i), \tag{4}$$

where $r_i$ is the distance measured from the center of bubble $i$. This pressure equation can be given from the continuity and Euler equations of fluid flow (see, e.g., Refs. [7,18]), and is in the following used to examine the acoustic signal from the bubbles. Time-delay effects [24] due to the finite sound speed of water are neglected, but a remark will be made on a consequence of it. As a first approximation we neglect the translational motion of bubbles due to the secondary Bjerknes force (an interaction force proportional to $D_{ij}^{-2}$) [25], that is, assuming $dD_{ij}/dt=0$. Hence, we set $D_{ij}$ to be much larger than $R_{i0}$ ($D_{ij}\approx10R_{i0}$) and consider only the first few periods of bubble oscillation, in which the translational velocity should be very small. As demonstrated below, the first one or two periods are sufficient for our discussion.

## III. RESULTS AND DISCUSSIONS

First we consider a single-bubble case to confirm that single bubbles can emit positive pulses only. The radius-time curves for two different bubbles of $R_{10}=10\ \mu\mathrm{m}$, $R_{20}=15\ \mu\mathrm{m}$ with $D_{12}=\infty$ are shown in Fig. 1(a). Here, we set the initial condition as $R_i(t=0)=0.13R_{i0}$ and $\dot{R}_i(t=0)=0$ in order to simulate the highly compressed state of the microbubbles at their generation. Due to the high internal pressure, the bubbles undergo rapid expansion and reach a maximum size of about $2.5R_{i0}$. Then they collapse and rebound many times. The oscillation amplitudes decrease monotonically in time due to the viscosity and compressibility of water. The pressure waves from the bubbles measured at $r_1=r_2=30R_{10}$ are shown in Fig. 1(b). From this, one knows that the single bubbles can emit positive pulses only. Between the positive pulses, one finds low-amplitude negative pressures, which resulted from a weak deceleration of the bubble surface acting when $R_i(t)>R_{i0}$. Their amplitudes (and also fundamental frequencies) are, however, obviously much lower than those of the positive pulses and hence they are incapable of explaining the negative pulses in the acoustic signal. The positive pulses are produced at the bubble collapse where the bubble surface is strongly accelerated [i.e., $\ddot{R}_i$ in Eq. (4) has a very large value]. However, from Eq. (4) one finds that to produce a negative pulse the bubble surface needs to be strongly decelerated: this may be impossible when only single bubbles are considered.

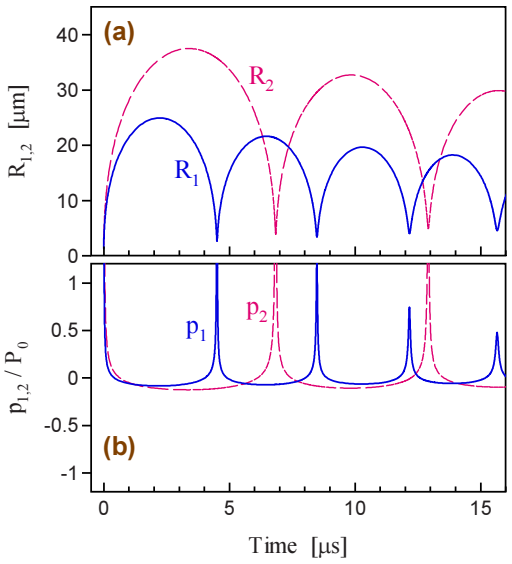


FIG. 1. (Color online) Bubble radii $R_{1,2}$ (a) and emitted pressures $p_{1,2}$ measured at $r_{1,2}=30R_{10}$ (b) in a single-bubble case ($D_{12}=\infty$) as functions of time. The ambient radii of the bubbles are $R_{10}=10\ \mu\mathrm{m}$ and $R_{20}=15\ \mu\mathrm{m}$. The solid and dashed lines are for bubbles 1 and 2, respectively. The pressures are normalized by the atmospheric pressure $P_0$. Only positive pulses are found in $p_{1,2}$.

This difficulty is resolved by considering bubble-bubble interaction. As is well known, when a pressure wave propagating in water hits the water-air interface, most of its energy is reflected and a reflected wave is produced whose phase is opposite to that of the incident wave. This is because air's acoustic impedance is much smaller than that of water. It is also known that negative pressure waves generated when strong positive pulses from collapsing bubbles hit a water-air interface can be strong enough to cause secondary cavitation [26]. Since the surface of gas bubbles considered here is also a free surface, it would be able to produce negative pulses. In Fig. 2, we show a result for a double-bubble case. Here, we

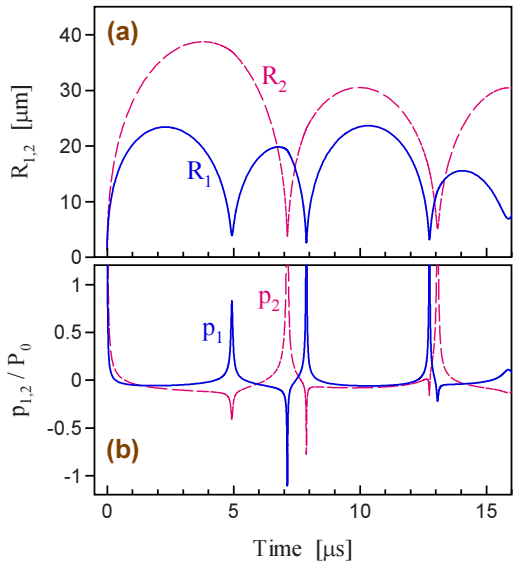


FIG. 2. (Color online) Same as Fig. 1, but in a double-bubble case ($D_{12}=10R_{10}$). Both positive and negative pulses are found in $p_{1,2}$, as in the broadband noise reported in Ref. [1].

used the same parameters as in the above example except for $D_{12}=10R_{10}$. In this case, the change of oscillation amplitude is nonmonotonic because of the modulation effect due to bubble-bubble interaction. In the bubble-emitted pressures presented in Fig. 2(b), in contrast to the single-bubble case, not only positive pulses but also negative pulses appear. In order to confirm the robustness of this observation, we performed a parametric study. The result is presented in Fig. 3, where the maximum amplitudes of the negative pulses for $R_{10}=10$ $\mu$m and $D_{12}=10R_{10}$ are shown as functions of $R_{20}$. This proves that strong negative pulses are emitted in most cases. From this figure it is also found that the maximum amplitudes have a complicated dependence on the ambient radius. The radius-time and pressure-time curves for $R_{20}=6$ $\mu$m and $R_{20}=10$ $\mu$m are shown in Figs. 4 and 5, respectively. For $R_{20}=6$ $\mu$m, negative pulses are found but their amplitudes are very low. For $R_{20}=10$ $\mu$m (i.e., $R_{20}=R_{10}$), no negative pulses are found, implying that systems of identical bubbles do not emit negative pulses.

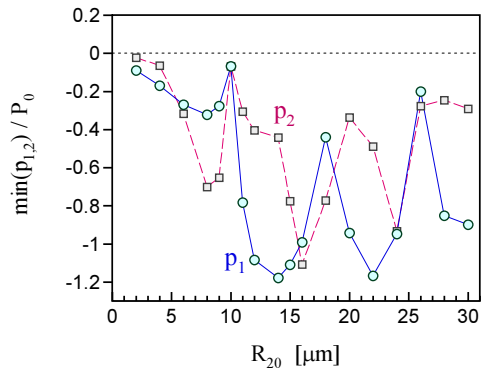


FIG. 3. (Color online) Maximum amplitudes of the negative pulses normalized by $P_0$ $[\min(p_{1,2})/P_0]$ as functions of $R_{20}$. $R_{10}$ and $D_{12}$ are fixed to 10 $\mu$m and $10R_{10}$, respectively. The circles and squares are for bubbles 1 and 2, respectively.

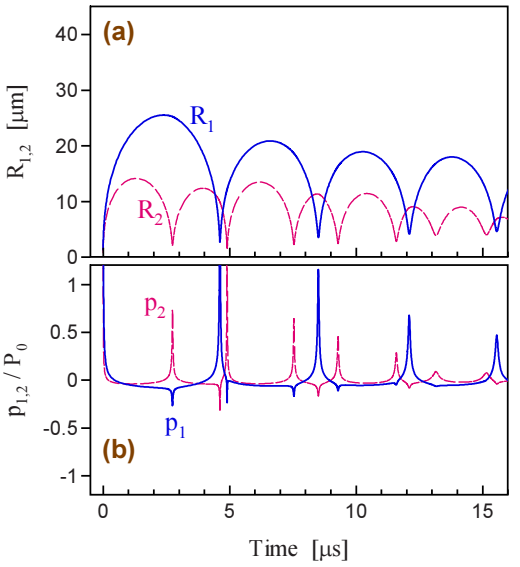


FIG. 4. (Color online) Same as Fig. 2, but for $R_{10}=10$ $\mu$m and $R_{20}=6$ $\mu$m.

The frequency spectra for $R_{10}=10$ $\mu$m and $R_{20}=15$ $\mu$m taken from $p_1/P_0$ and $p_2/P_0$ in Figs. 1(b) and 2(b) are shown in Fig. 6. All of the presented spectra show a broad distribution. The peak frequencies in the single-bubble case are 0.287 MHz for $p_1$ and 0.185 MHz for $p_2$, which are roughly the same as the repetition rates of the positive pulses deduced from Fig. 1(b) (about 0.27 and 0.17 MHz, respectively). We found several qualitative differences between the spectra in the single- and double-bubble cases. One of the differences is clearly seen in Fig. 7, which shows the spectra in a frequency range around the peak frequencies. The spectrum of $p_1$ in the double-bubble case has a more complex structure than that in the single-bubble case, particularly in a frequency range between 0.1 MHz and 1 MHz: A number of characteristic peaks are added and the spectrum structure be-

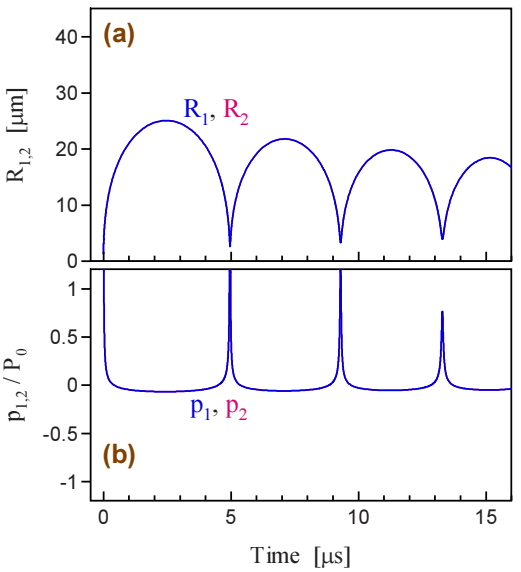


FIG. 5. (Color online) Same as Fig. 2, but for $R_{10}=R_{20}=10$ $\mu$m.

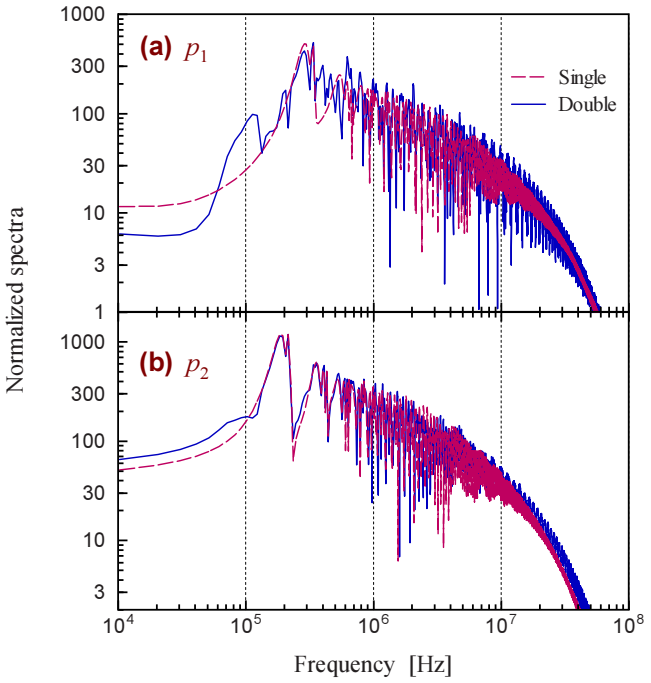


FIG. 6. (Color online) Frequency spectra of $p_1/P_0$ (a) and $p_2/P_0$ (b) for $R_{10}=10$ $\mu$m and $R_{20}=15$ $\mu$m. The dashed and solid curves are for the single- and double-bubble cases, respectively. The spectra were generated using the data shown in Figs. 1(b) and 2(b) in a time period from $t=2.5$ to 100 $\mu$s. The sampling frequency assumed is 500 MHz.

comes much denser through the bubble-bubble interaction. Compared to $p_1$, the change in the spectrum of $p_2$ is small: No qualitative differences are found between $p_2$ in the single- and double-bubble cases. This suggests that the larger bubble (bubble 2) has a more significant influence on the neighboring bubble and the dynamics of the neighboring smaller bubble (bubble 1) is thus changed more drastically (the same tendency is found also in systems of linearly oscillating bubbles in a sinusoidal sound field [10]). When $R_{10}=R_{20}=10$ $\mu$m, the difference between the spectra in the single- and double-bubble cases is very small, as can be expected from the above observation that only positive pulses are emitted for $R_{10}=R_{20}$; see Fig. 8. The peak frequency is decreased by bubble-bubble interaction, which appears to be consistent with the fact that the natural frequency of identical bubbles oscillating in phase each other is lower than that of the individual bubbles [12,14,27].

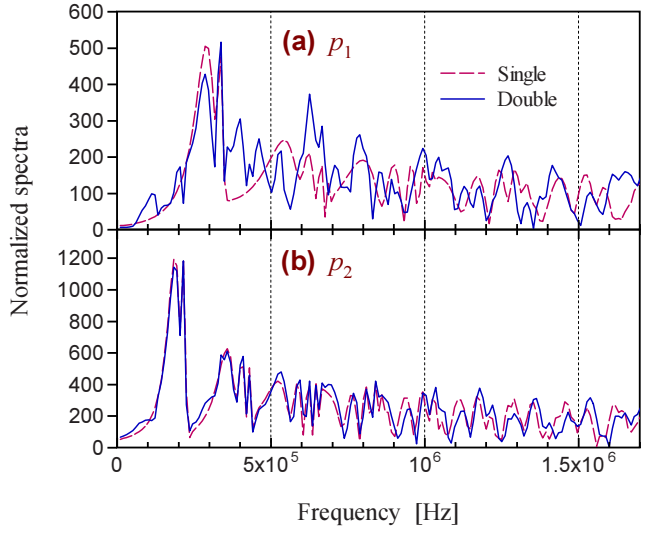


FIG. 7. (Color online) Frequency spectra of $p_1/P_0$ (a) and $p_2/P_0$ (b) for $R_{10}=10$ $\mu$m and $R_{20}=15$ $\mu$m in a frequency range around the peak frequencies.

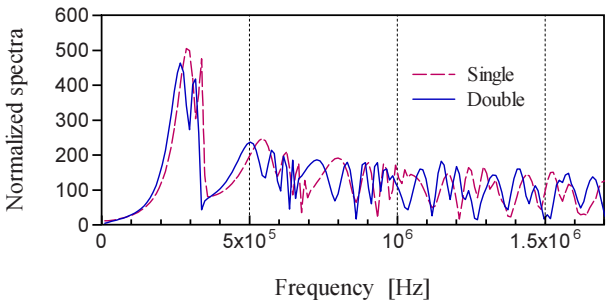


FIG. 8. (Color online) Same as Fig. 7, but for $R_{10}=R_{20}=10$ $\mu$m.

Let us consider how the negative pulses were produced. As can be seen in Fig. 2(b), the negative pulses from a bubble coincide with the positive pulses emitted by the other bubble at its collapse. This observation tells us that the negative pulses are produced when the positive pulses hit the surface of the neighboring bubble. Shown in Fig. 9 is a close-up view of $p_1$ and $R_1$ in Fig. 2 around the time ($t\approx 7$ $\mu$s) of the first negative pulse from bubble 1. The figure also shows the inertia and acceleration portions of $p_1$, that is,

$$\alpha_1 = \frac{2\rho R_1 \dot{R}_1^2}{r_1} \tag{5}$$

and

$$\beta_1 = \frac{\rho R_1^2 \ddot{R}_1}{r_1}. \tag{6}$$

One can see that the surface of bubble 1 is strongly decelerated in the period when it emits the negative pulse, though no noticeable disturbance is seen in $R_1$ because the duration of the deceleration is very short. This strong deceleration is clearly caused by the strong positive pulse from bubble 2, which impulsively compresses bubble 1. Deceleration is also observed in a following period where the bubble is shrinking, but no negative pressure is found because a large inertia ($\alpha_1$) cancels the effect from the deceleration ($\beta_1$).

In order to more deeply understand the mechanism of negative pulse generation, we perform theoretical studies based on the coupled Keller-Miksis equations. First, we consider the relation between the amplitudes of the incident and reflected pulses. If $R_1 \gtrsim R_{10}$ (i.e., $p_{b,1} \lesssim P_0$) and $\dot{R}_1 \ll c$ at the time of collapse of bubble 2, where $\ddot{R}_2$ has a very large value, only the acceleration terms in Eq. (1) may be significant for bubble 1 and the remaining terms are thus negligible. Hence, the equation and also Eq. (4) are reduced to

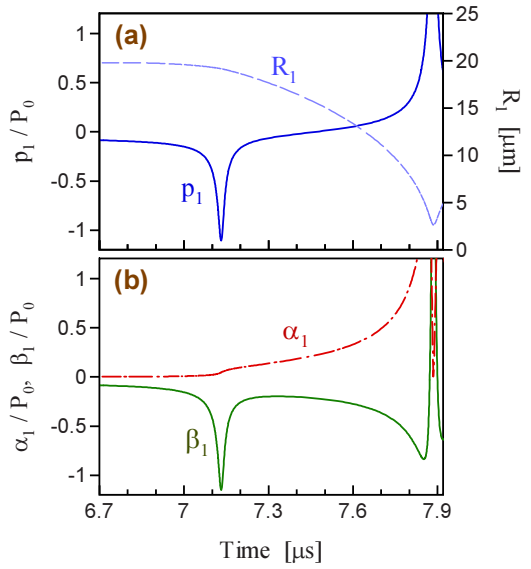


FIG. 9. (Color online) (a) Close-up view of $p_1$ and $R_1$ in Fig. 2 around the time of the first negative pulse from bubble 1, and (b) inertia ($\alpha_1$) and acceleration ($\beta_1$) portions of $p_1$ in the same period. $p_1$, $\alpha_1$, and $\beta_1$ are normalized by $P_0$.

$$\left(1+\frac{1}{A_R}\right)R_1\ddot{R}_1 = -\frac{1}{D_{12}}R_2^2\ddot{R}_2, \tag{7}$$

$$p_i = \frac{\rho}{r_i}R_i^2\ddot{R}_i \quad \text{for } i=1,2. \tag{8}$$

In Eq. (7), $A_R$ is an acoustic Reynolds number defined here as

$$A_R \equiv \frac{\rho c R_1}{4\mu}. \tag{9}$$

Since $A_R$ is much larger than unity ($A_R \simeq 973$ for $R_1 = 2.6$ $\mu$m, a typical minimum radius at collapse), Eq. (7) is further reduced to

$$R_1\ddot{R}_1 = -\frac{1}{D_{12}}R_2^2\ddot{R}_2. \tag{10}$$

If one measures $p_1$ and $p_2$ at the same distance from the corresponding bubbles (i.e., $r_1=r_2$), Eq. (10) is rewritten using Eq. (8) as

$$p_1 = -\frac{R_1}{D_{12}}p_2. \tag{11}$$

Equation (10) proves that $\ddot{R}_1$ has the opposite sign from that of $\ddot{R}_2$, that is, the surface of bubble 1 is strongly decelerated at the moment when bubble 2 collapses, where the surface of bubble 2 is strongly accelerated due to its high internal pressure. From Eq. (11), one finds that the ratio between $p_1$ and $p_2$ is simply determined by $-R_1/D_{12}$, and that the amplitude of the negative reflected pulse is large if $R_1$ is large when the pressure pulse from bubble 2 hits bubble 1. The numerical result shown in Fig. 2(b) gives $p_1/p_2=-0.200$ and $-R_1/D_{12}=-0.192$ for the first negative pulse from bubble 1 (at $t\simeq 7$ $\mu$s), and $p_2/p_1=-0.243$ and $-R_2/D_{12}=-0.231$ for the second negative pulse from bubble 2 ($t\simeq 8$ $\mu$s), both of which reveals a reasonable agreement. However, Eq. (11) gives a less accurate result for the first negative pulse from bubble 2 ($t\simeq 5$ $\mu$s): $p_2/p_1=-0.507$ but $-R_2/D_{12}=-0.369$. This may be because $p_1$ and $p_2$ are not large enough to fully satisfy the assumptions used in deriving Eq. (10).

Next, we consider what occurs when $R_{10}=R_{20}$. As shown in Fig. 5, no negative pulses are emitted for $R_{10}=R_{20}=10$ $\mu$m, although strong positive pulses are emitted which definitely hit the neighboring bubble. Here we attempt to explain this observation. For $R_{10}=R_{20}$ and $R_1=R_2$, at the final stage of bubble collapse where $\ddot{R}_1$ and $p_{b,1}$ are very large and $\dot{R}_1 \simeq 0$, Eq. (1) may be reduced to

$$\rho R_1\ddot{R}_1 = p_{b,1} - \rho\left(\frac{1}{A_R}+\frac{R_1}{D_{12}}\right)R_1\ddot{R}_1, \tag{12}$$

where we neglected the surface-tension and viscous forces and $P_0$ since their magnitudes should be much smaller than the internal pressure $p_{b,1}$. Since $1/A_R$ ($\simeq 1/977$ for $R_1=2.61$ $\mu$m at the first collapse) is much smaller than $R_1/D_{12}$ ($\simeq 1/38$), Eq. (12) is further reduced to

$$\rho R_1\ddot{R}_1 = p_{b,1} - \frac{\rho}{D_{12}}R_1^2\ddot{R}_1. \tag{13}$$

From this we have

$$\ddot{R}_1 = \frac{p_{b,1}}{\rho R_1\left(1+\frac{R_1}{D_{12}}\right)}. \tag{14}$$

This says that $\ddot{R}_1$ is positive at the bubble collapse and hence the bubbles emit positive pulses. This conclusion is consistent with the above numerical finding and is not altered even if $1/A_R$ is considered.

This result comes from the fact that, in the considered case where the bubbles collapse at the same time, the sound pressure $(\rho/D_{12})R_1^2\ddot{R}_1$ from the neighboring bubble cannot exceed the bubbles' internal pressure $p_{b,1}$. The sound pressure generated by bubble 2, whose internal pressure is $p_{b,1}$, must be smaller than $p_{b,1}$ when it is measured at the position of bubble 1, because the bubbles are separated by a finite distance $D_{12}$. Since the internal pressure of bubble 1 is also $p_{b,1}$, it is not exceeded by the sound pressure, and the right-hand side of Eq. (13) is thus positive: in other words, bubble 1 emits a strong positive pulse, resulting from the high internal pressure, whose absolute amplitude is greater than that of the negative reflected pulse. This finding suggests that the bubble surface, a free surface, does not always produce negative reflected pulses and the characteristics of the reflected waves depend on the state of the gas in the bubbles. The negative pulses found in Figs. 2(b) and 4(b) are produced because the positive pulses hit the neighboring bubble when its internal pressure is not high.

## IV. SUMMARY

We have studied the interaction of microbubbles through pressure pulses to suggest a possible origin of the negative

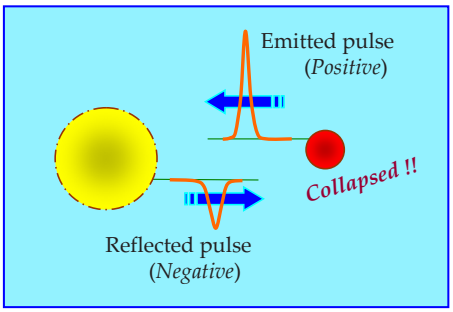


FIG. 10. (Color online) Noise generation process. Positive pressure pulses are emitted by collapsed bubbles (the right circle) and propagate through the surrounding liquid. The positive pulses generate negative reflected pulses when they hit and impulsively compress neighboring bubbles (the left circle). The positive and negative pulses will make up a cavitation noise. Note that the pulse profiles shown represent those measured at a fixed location, as functions of time. The wavelengths of the pulses are much larger than the bubble radii.

pulses found in broadband cavitation noise. The proposed scenario of noise generation is summarized as follows. When a large cavitation bubble collapses and fragments, a number of microbubbles are formed [1]. The microbubbles expand rapidly and then collapse to emit positive pressure pulses (the right half of Fig. 10). The positive pulses hit and impulsively compress neighboring bubbles to cause a brief but strong deceleration of the bubble surface. This deceleration, which creates a strong tension in the surrounding liquid, produces negative reflected pulses (the left half of Fig. 10), and then a signal consisting of positive and negative pulses is generated. If the time-delay effect is considered, the positive and associated negative pulses are measured with a time interval determined by the relative position of the bubbles and the sound speed or shock-wave velocity of water (which can greatly increase in the vicinity of collapsing bubbles [22,28]). Spectral analysis has revealed that the frequency spectrum of the cavitation noise, particularly from the smaller bubble in a double-bubble system, becomes much more complicated and denser by bubble-bubble interaction. Though only a few negative pulses were observed in the double-bubble cases studied here, consideration of a larger number of bubbles and multiple scattering of sound may allow us to explain the large number of pressure pulses found in the recorded broadband noise.

Discussing further details of the noise generation process, we have revealed that the amplitudes of the negative reflected pulses depend on the instantaneous radius and the state of the internal gas of the reflecting bubble. Interestingly, no negative pulses are generated when a system of identical bubbles is considered. This is because the positive pulse from a bubble hits the neighboring bubble just when it collapses, at which moment the bubble's internal pressure is higher than the pressure of the incident positive pulse. This observation suggests that the surface of gas bubbles, a free surface, does not always produce a negative reflected pulse, and also that negative pulses cannot be described by theoretical models that consider only systems of identical bubbles (the last conclusion may be altered in cases of large time delays, where positive pulses from a bubble hit the other bubble after its internal pressure has decreased considerably). The presented findings would be useful in understanding not only the shrimp-emitted acoustic signal but also other types of cavitation noise found, e.g., in fluid machinery [3,4] and medical applications [29].

Lastly, we make some remarks on the limitations of the present work. The present study was based on several crude simplifications, such as the drastic reduction of the number of microbubbles and the assumption of spherical symmetry of bubbles. All of those simplifications must result in quantitative errors. As is known, the natural frequency of bubble clouds depends on the number density of bubbles [4], and hence the artificial reduction of the number of bubbles should cause inaccuracy in predicting the noise characteristics (e.g., the repetition rate of the pressure pulses). Spherical symmetry can be strongly broken, particularly when closely interacting bubbles collapse, where jetting and even bubble fragmentation occur [30], both of which must alter the noise characteristics. A more realistic model that can represent such complicated processes is needed to achieve a more accurate description of cavitation noise.

## ACKNOWLEDGMENTS

This work was partially supported by the Ministry of Education, Culture, Sports, Science, and Technology of Japan through a Grant-in-Aid for Young Scientists (B) (No. 20760122) and by the Japan Society for the Promotion of Science through a Grant-in-Aid for Scientific Research (B) (No. 20360090).

[1] M. Versluis, B. Schmitz, A. von der Heydt, and D. Lohse, Science **289**, 2114 (2000).
[2] Similar acoustic signals from cavitation bubbles can be found also in different fields; see, e.g., Refs. [3,4].
[3] S. Kumar and C. E. Brennen, J. Fluid Mech. **255**, 541 (1993).
[4] C. E. Brennen, *Cavitation and Bubble Dynamics* (Oxford University Press, New York, 1995).
[5] V. F. K. Bjerknes, *Fields of Force* (Columbia University Press, New York, 1906).
[6] E. A. Zabolotskaya, Sov. Phys. Acoust. **30**, 365 (1984).
[7] R. Mettin, I. Akhatov, U. Parlitz, C. D. Ohl, and W. Lauterborn, Phys. Rev. E **56**, 2924 (1997).
[8] A. A. Doinikov, J. Acoust. Soc. Am. **111**, 1602 (2002).
[9] M. Ida, Phys. Rev. E **67**, 056617 (2003).
[10] M. Ida, Phys. Fluids **17**, 097107 (2005).
[11] I. Akhatov, U. Parlitz, and W. Lauterborn, Phys. Rev. E **54**, 4990 (1996).
[12] A. Shima, J. Basic Eng. **93**, 426 (1971).

[13] I. Tolstoy, J. Acoust. Soc. Am. **80**, 282 (1986); C. Feuillade, *ibid.* **98**, 1178 (1995).
[14] M. Ida, Phys. Lett. A **297**, 210 (2002); J. Phys. Soc. Jpn. **71**, 1214 (2002).
[15] M. Ida, Phys. Rev. E **72**, 036306 (2005).
[16] Z. Ye and A. Alvarez, Phys. Rev. Lett. **80**, 3503 (1998); M. Kafesaki, R. S. Penciu, and E. N. Economou, *ibid.* **84**, 6050 (2000).
[17] M. Ida, T. Naoe, and M. Futakawa, Phys. Rev. E **75**, 046304 (2007).
[18] M. Ida, T. Naoe, and M. Futakawa, Phys. Rev. E **76**, 046309 (2007).
[19] R. Löfstedt, B. P. Barber, and S. J. Putterman, Phys. Fluids A **5**, 2911 (1993).
[20] W. C. Moss, J. L. Levatin, and A. J. Szeri, Proc. R. Soc. London, Ser. A **456**, 2983 (2000).
[21] S. Fujikawa and T. Akamatsu, J. Fluid Mech. **97**, 481 (1980); Y. Matsumoto and F. Takemura, JSME Int. J., Ser. B **37B**, 288 (1994); K. Yasui, Phys. Rev. E **56**, 6750 (1997); B. D. Storey and A. J. Szeri, Proc. R. Soc. London, Ser. A **456**, 1685 (2000); R. Toegel and D. Lohse, J. Chem. Phys. **118**, 1863 (2003).
[22] J. Holzfuss, M. Rüggeberg, and A. Billo, Phys. Rev. Lett. **81**, 5434 (1998).
[23] S. W. Karng, Y. P. Lee, K.-Y. Kim, and H.-Y. Kwak, J. Korean Phys. Soc. **43**, 135 (2003).
[24] S. Fujikawa and H. Takahira, Acustica **61**, 188 (1986); A. A. Doinikov, R. Manasseh, and A. Ooi, J. Acoust. Soc. Am. **117**, 47 (2005).
[25] A. A. Doinikov, Phys. Rev. E **64**, 026301 (2001); N. A. Pelekasis, A. Gaki, A. Doinikov, and J. A. Tsamopoulos, J. Fluid Mech. **500**, 313 (2004), and references therein.
[26] Y. Tomita, T. Kodama, and A. Shima, Appl. Phys. Lett. **59**, 274 (1991); D. Obreschkow, P. Kobel, N. Dorsaz, A. de Bosset, C. Nicollier, and M. Farhat, Phys. Rev. Lett. **97**, 094502 (2006); E. Robert *et al.*, Phys. Fluids **19**, 067106 (2007).
[27] S. T. Zavtrak, Sov. Phys. Acoust. **33**, 145 (1987).
[28] R. Pecha and B. Gompf, Phys. Rev. Lett. **84**, 1328 (2000).
[29] J.-L. Mestas *et al.*, Proc.-IEEE Ultrason. Symp. **3**, 1816 (2004); Y. Liu *et al.*, J. Acoust. Soc. Am. **118**, 3328 (2005); Y. Liu *et al.*, *ibid.* **120**, 492 (2006).
[30] Yen-Hung Chen and Lin I, Phys. Rev. E **77**, 026304 (2008), and references therein.